Estimating the potential for solar energy utilization in Chile by satellite-derived data and ground station measurements

Rodrigo A. Escobar [a],[*], Cristián Cortés [b], Alan Pino [b], Marcelo Salgado [b],
Enio Bueno Pereira [c], Fernando Ramos Martins [c], John Boland [d], José Miguel Cardemil [e]

[a] *Escuela de Ingeniería, Pontificia Universidad Católica de Chile, Vicuña Mackenna 4860, Santiago, Chile*
[b] *Fraunhofer Chile Research, Center for Solar Energy Technologies, Santiago, Chile*
[c] *Centro de Ciência do Sistema Terrestre—Instituto Nacional de Pesquisas Espaciais (Earth System Center—National Institute for Space Research),
São José dos Campos, Brazil*
[d] *School of Information Technology and Mathematical Sciences, University of Southern Australia, Audelaide, Australia*
[e] *Universidad Diego Portales, Escuela de Ingeniería Industrial, Santiago, Chile*

Abstract

The progress in solar energy resource assessment for Chile is reported, including measurements from a ground station network spanning more than three years of data, satellite estimations from the recently developed Chile-SR model including three full years of data, and simulations that evaluate the potential for solar thermal, photovoltaics (PV) and concentrated solar power (CSP) utilization.

The satellite estimation model adapts the Brasil-SR methodology with the combined use of visible and infrared (IR) satellite images, an enhanced treatment for altitude-corrected meteorological variables and an effective cloud cover computations that allows the estimation of the global horizontal and diffuse horizontal irradiation on an hourly basis. Direct normal irradiation (DNI) is computed from the direct horizontal irradiation by applying the Boland–Ridley–Laurent (BRL) model of diffuse fraction and proper solar geometry corrections. Comparison of the satellite-derived data with the ground station data shows good agreement and low error levels thus served for model validation. The results indicate that Chile is endowed with one of the highest levels of solar resource in the world in terms of annual irradiation for large portions of its territory. There is a small decrease in yearly levels of GHI and DNI with latitude that in practice indicate that most of the country shares exceptional conditions for solar energy. However, coastal regions have a large decrease in both GHI and DNI due to the persistence of seasonal cloud covers with daily cycles.

The use of irradiation data from the Chile-SR model for system simulation indicates that solar fractions over 80% are achievable for residential-sized solar thermal systems in most of the country, with PV systems yielding between 4.5 and 8 kW h/kWpv, and CSP annual yields of up to 240 GW h/year for a 50 MW parabolic trough plant. These results indicate that the country has the potential for ample utilization of solar energy conversion technologies in most of its territory when considering annual GHI and DNI, suitable terrain availability and energy (electricity and heat) demand from industrial, commercial and residential activities.
© 2015 Elsevier Ltd. All rights reserved.

Keywords: Solar resource assessment; Chile; Ground measurements; Satellite estimation; Cloud cover estimation

* Corresponding author at: Escuela de Ingeniería, Pontificia Universidad Católica de Chile, Vicuña Mackenna 4860, Santiago, Chile. Tel.: +56 23545478.
  E-mail address: rescobar@ing.puc.cl (R.A. Escobar).

1. Solar energy in Chile

Renewable energy promotion in Chile has obtained government support by means legislations that mandate a renewable energy quota of up to 10% of the electrical energy generated, which must be met by 2024, with public announcements already being made that would modify this goal in order to achieve 20% of power generation by 2020 from renewable energy (Ministerio de Economía de Chile, 2007). This plan has sparked interest in introducing renewable energy systems to the country's electricity system. Solar energy is currently at the initial stages of market penetration, with several projects being developed including PV, CSP, and industrial heat supply plants. However, several barriers still exist and among them is the absence of a valid solar energy database available to the public, adequate for energy system simulation and planning activities. Even as the country is endowed with an exceptional solar potential, the contribution of solar energy to the energy mix in Chile is still small. As of June 2015, only 537 MW of PV plants have been deployed and are currently operating with 1849 MW being built and 8990 MW approved for construction in the environmental evaluation system. There are 110 MW of CSP plants under construction with another 870 approved (CIFES, 2014). Regarding solar heating and cooling systems, statistics from the *Solar Heat Worldwide* report from International Energy Agency indicate that as of 2013 there was 139,309 m^2 of installed solar thermal collectors for both the residential and commercial sectors (MAuthner et al., 2015). In terms of energy contribution, statistics from the government indicate that during 2014 a total of 458 GW h were produced accounting for 0.66% of the total Chilean electricity consumption, and that from January to May 2015 the contribution amounted to 484 GW h, or 1.65% of the national total for the period. There are currently no solar desalination projects in Chile. One of the several reasons that explain the difficulty in developing solar projects during the past years is the relatively scarce solar resource assessment activities that could allow reducing the risk associated to the evaluation of the energy yield of the solar plants in Chile. The efforts of our research team aim to produce and make available to the public and industry a proper set of solar radiation data able to allow project development with lower resource-related uncertainty.

Previous reports by the authors identified several databases of solar radiation that are publicly available for Chile and discussed their merits and shortcomings (Ortega et al., 2010; Escobar et al., 2014a). It has been found that significant deviation exists between sources, and that all ground station measurements display unknown uncertainty levels, thus highlighting the need for a proper country-wide long-term resource assessment initiative for the public domain. As the solar energy levels throughout the country are high according to all sources, it is thought that existing data is adequate for energy planning activities although not yet for proper power plant design and dimensioning.

However, there are several commercial products that are not freely available to the public. As a general conclusion, although for Chile there are several databases of ground measurements, a weather simulation model, and satellite-derived data, none of these locally-produced data sources are completely valid and therefore a nationwide effort of resource assessment was needed at the time our research started (Ortega et al., 2010).

This report presents a summary of the solar energy resource assessment activities conducted by the Pontificia Universidad Católica de Chile (PUC) supported by its collaborators from the Instituto Nacional de Pesquisas Espaciais (INPE) of Brasil, University of Southern Australia, Universidad Diego Portales, and Fraunhofer Chile Research, briefly recounting what was already presented in Escobar et al. (2014a) and expanding on what was presented there and also at the ISES Solar World Congress 2013 (Escobar et al., 2014b). In short, a network of ground stations has been deployed in locations of scientific interest such as high altitude places, salt lakes, snow covered terrain, and others. A modification to an existing satellite estimation model has been developed, building upon the Brasil-SR model partially developed by researchers at INPE, and introducing different treatments for the meteorological variables and the effective cloud cover computations. The report presents results and comparisons for the described data sources. Validation of the Chile-SR model indicates that the model is properly estimating solar radiation for the range of climates present in Chile, which allows utilizing its data for an initial estimation that highlights the large potential energy yields of a variety of solar energy conversion systems in Chile. Finally, the Chile-SR data is used for simulations that estimate the potential in Chile for solar thermal, PV, and CSP projects.

2. The PUC-FONDEF ground station network

The network of ground stations was deployed starting on 2010, consisting of 13 stations, 4 of which are designed and operated under the Baseline Surface Radiation Network (BSRN) standards, and the remaining 9 are of three

Table 1
Ground station network.

Station name	Type	Start date of operation
1. Arica	RSBR	01/08/2011
2. Pozo Almonte	RSBR	04/04/2012
3. Patache	RSBR	16/01/2013
4. Sur Viejo	RSBR	07/07/2011
5. Crucero	RSBR	16/01/2012
6. Coya Sur	RSBR	05/07/2011
7. San Pedro	Sun tracker	03/12/2010[*]
8. El Tesoro	RSBR	01/01/2009
9. Diego de Almagro	RSBR	02/08/2011
10. Santiago	Sun tracker	22/12/2010
11. Curicó	Sun tracker	01/06/2012
12. Talca	Sun tracker	09/08/2012
13. Marimaura	RSBR	12/07/2012

[*] Decommissioned on dec 2011.

Fig. 1. Northern and Central Chile, and the approximate locations of the ground stations of the UC-Fondef network.

different configurations of *Rotating Shadow Band Radiometers* (RSBR) from Irradiance Inc. Table 1 indicates the name, type, and start date of operation for the stations, whose approximate locations are displayed in the map as in Fig. 1. Most of the stations are also operated in agreement with industry and due to confidentiality issues the amount of information that can be shared such as exact location and data is limited. The stations that follow the

BSRN standards (König-Langlo et al., 2013; Hegner et al., 1998; McArthur, 2004) are composed of sun trackers, sun sensors for accurate positioning, pyranometers, heating and ventilation units, pyrgeometers, pyrheliometers, UV meters, and also temperature, atmospheric pressure, relative humidity, wind speed and direction sensors, all connected to dataloggers, with power supply from the grid. Although the stations are not part of BSRN, their operation follows its main guidelines (König-Langlo et al., 2013; Hegner et al., 1998; McArthur, 2004) for all relevant procedures as well as the maintenance activities. The basic configuration for the RSBR devices includes photoelectric radiometers, a motor controller and rotating shadow band, temperature, atmospheric pressure, relative humidity, wind speed and direction sensors, all connected to dataloggers, with power supply from a small-scale PV system. A second configuration lacks all meteorological sensors, for use in locations that already have a meteorological. A third configuration is similar to the first one, with the addition of a thermopile pyranometer for a redundant measurement of global horizontal radiation, which is used at sites where radiation conditions are particularly interesting and where local personnel is readily available for maintenance and cleaning of the thermopile pyranometer. Fig. 2 shows two different configurations of the ground stations: one RSBR, and one BSRN-designed station deployed in the field. These stations have the objective of supplying data that satisfies international standards and criteria for design, operation and maintenance, thus providing data for project developers and policymakers, and also for the Chile-SR satellite estimation model validation described in a following section. Calibration certificates for these stations are kept updated as the sensors are rotated with new ones, while it is planned to directly trace all sensors (old and new) to the world reference as suggested by international standards during 2015. Data qualification algorithms have been adapted and transferred from INPE to PUC for analyzing the quality of data from the stations.

According to JCGM (2008), Reda (2011), Myers et al. (2001), Habte et al. (2014) it is possible to evaluate the uncertainty associated to field solar radiation measurements by considering the type of sensor, calibration, zenith response, spectral response, nonlinearity, temperature response, aging per year, datalogger accuracy, and maintenance. Using the GUM methodology (Habte et al., 2014) it is possible to estimate that for the thermopile sensors the uncertainty is up to 4% for GHI and 2.5% for DNI, while for the photodiode sensors uncertainty is 5%. Laboratory and field comparisons for GHI and DNI measured with thermopile sensors and with RSBR devices showed good accuracy, with deviations no larger than 2% from the thermopile values for the RSBR data.

Fig. 3 shows hourly totals of GHI and DNI for each day of 2012 at four different sites: Crucero, (22°2S, 69°5W), Patache (20°8S, 70°1W), Santiago, located at (33°4S, 70°6W), and Curicó (34°5S, 71°1W). Crucero is a large desert plain located in extremely arid conditions that has seen interest

Fig. 2. RSBR station in Crucero and one station with tracker, pyrheliometer, and pyranometers in Talca.

from both the PV and CSP industries. Patache is a coastal site in a microclimate called *fog oasis* where a phenomenon of a local stratocumulus cloud enters the desert from the sea and creates a thick fog that allows a rich ecosystem to develop while greatly decreasing available radiation (Cereceda et al., 2008). Santiago is the capital city of Chile with a population of 6 million, located in a relatively dry Mediterranean climate and with episodes of heavy aerosol and particle pollution during winter. Curicó is a small city inserted in an agricultural region just 200 km south of Santiago that shares a similar climate although not the heavy urban pollution. These locations have been selected as they are representative of the conditions present in coastal, northern and central Chile in places of relevance in terms of energy demand for the mining industry (Crucero), residential and commercial sectors (Santiago), and for agricultural zones (Curicó). Patache is of interest as it shares the climate of the largest cities in coastal northern Chile and helps characterize the coastal clouds locally known as *camanchaca* that can affect solar plants located in the desert near the coast.

In Fig. 3 it can be observed that Crucero, with a yearly total of 2571 kW h/m^2 for GHI and 3389 kW h/m^2 for DNI as measured in 2012 is one of the top worldwide sites for solar radiation. Most of northern Chile shares this high radiation endowment as presented and discussed in Fig. 6. The seasonality for GHI is apparent, with shorter days and lower values for the winter season. However, during February there are episodes of persistent cloud covers resulting from moisture coming from the amazon basin in what is known as altiplanic winter. Even then, more than 300 days of clear skies are available each year. This is also apparent in the DNI plot for Crucero, where it can be seen that a large number of days have high DNI during most of the

day, with only a few low-DNI days occurring during altiplanic winter and seasonal winter.

Patache, although close to Crucero, is not located in the intermediate depression of Chile but on the edge of the megacliff that rises from sea level up to 1000 m in less than 2 km from the coastal line. The yearly totals are 2114 kW h/m^2 for GHI and 1908 kW h/m^2 for DNI. Its climate is very similar to that shared by the major cities in northern Chile and thus useful to gain insight on the potential for solar energy supply to the residential and commercial sectors that concentrate most of the population. In terms of radiation, this northern coastal climate is characterized by clear skies from December to April, with presence of cloud covers causing variability with decreased GHI and DNI the rest of the year. Thus, even as the two places are closely located, Crucero and Patache show how the coastal and desert climates of northern Chile have very different solar resource availability. This implies that different technology solutions for solar energy production will be required according to the particular characteristic of northern Chile main climate and microclimate regions.

The solar resource variability in Santiago and Curicó is higher due to their Mediterranean climate with occurrences of cloudy and clear days throughout the year with a strong summer/winter seasonality. Episodes of persistent cloud covers during several days are common during the year although less common in summer. In winter, cloud covers are more common, days are shorter, and radiation levels are greatly reduced. The yearly totals are 1913 kW h/m^2 for GHI and 1911 kW h/m^2 for DNI in Santiago, and 1791 kW h/m^2 for GHI and 1952 kW h/m^2 for DNI in Curicó. What is interesting to note is that even as the maximum distance between Crucero and Santiago is slightly less than 1600 km, in clear days the GHI and DNI have
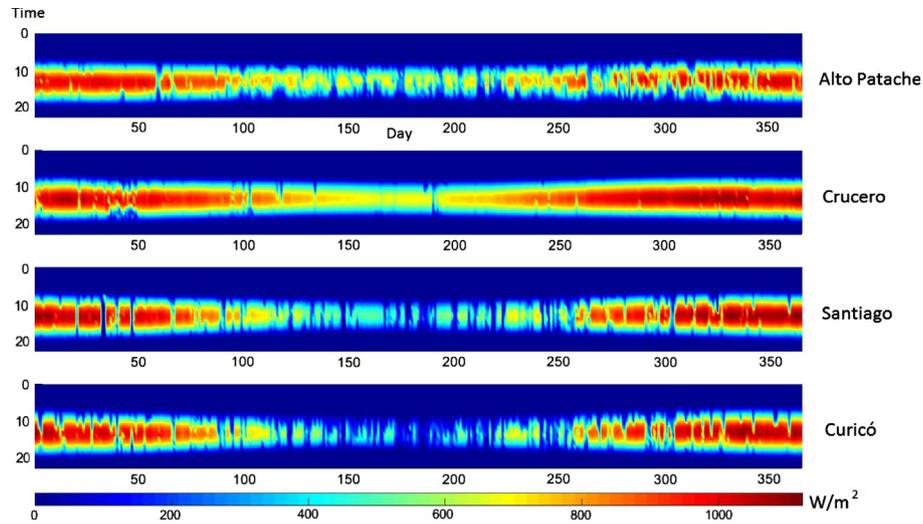
(a) Global Horizontal Irradiance GHI
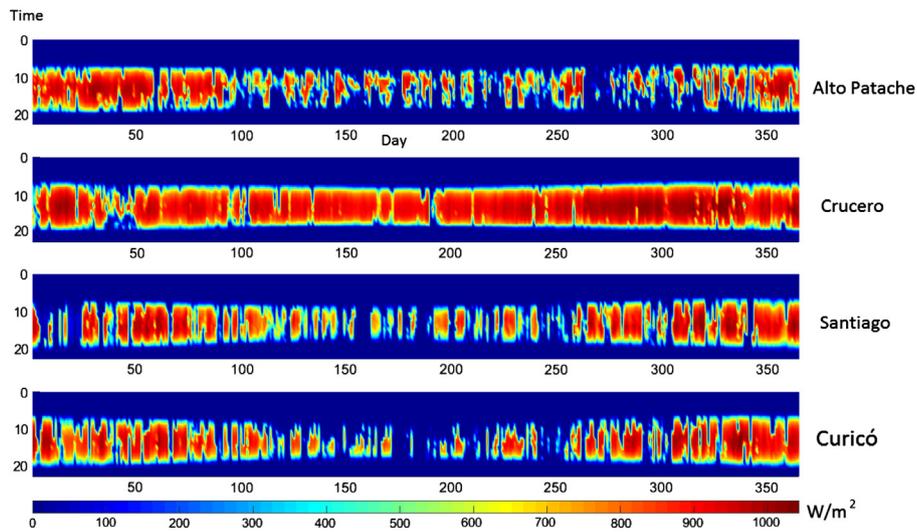
(b) Direct Normal Irradiance DNI

Fig. 3. Daily totals of solar radiation from January to December 2012 at four different locations.

very similar profiles and maximum levels that are only slightly reduced by the effects of latitude and altitude. However, the difference between desert and coast is much larger and the yearly total in Patache for DNI is closer to Santiago than to Crucero.

3. Chile-SR satellite-based estimation model

Ground measurement campaigns, although accurate, are expensive and prone to equipment failure, with poor maintenance leading to data of high uncertainty. Satellite estimation is cheaper yet sufficiently accurate, and it covers a large geographical area with adequate spatial and temporal resolution. Based on this, the authors aimed at developing a satellite estimation model that could produce accurate and low-uncertainty data for Chile by taking into account the different climatic characteristics in the country,

with enough spatial and temporal resolution to be used for project development. The Chile-SR model has been developed as a modification of the existing Brasil-SR model (Pereira et al., 2006; Martins et al., 2008, 2007; Ruther et al., 2008) developed by INPE, taking its basic algorithm and modifying it in order to create an adaptation especially suited for the largely different conditions that Chile presents: the Atacama desert located in its northern regions, then a mediterranean climate found in the country's central region, and finally a cold forest in its southern regions. All along the country, there are also the coastal, interior, and mountainous zones. The objective is then for the model to be able to capture all these climates and provide accurate estimations of the solar irradiation.

Fig. 4 shows a summarized description of the Chile-SR model, its inputs, the atmospheric parameterization, and related outputs. The model considers that the main
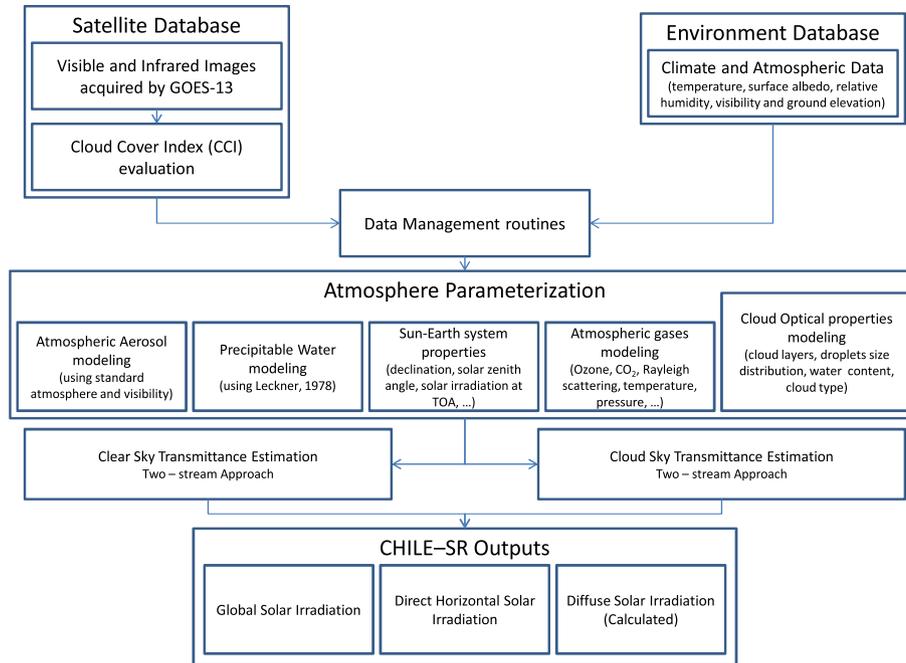
Fig. 4. General description of the Chile-SR model.

modulator of solar radiation at earth's surface is the cloud cover, while in absence of cloud covers the modulator becomes the aerosol column that determines the atmospheric radiative transmittance. The Chile-SR model estimates the incident radiation at the surface utilizing a two-flow methodology that calculates a clear-sky atmospheric transmittance τ_{clear} and a cloudy-sky atmospheric transmittance τ_{cloud}. While τ_{clear} is a function of the surface albedo, zenith angle and aerosol optical depth, τ_{cloud} depends mostly on the cloud optical properties. Both atmospheric transmittance components are estimated using the input meteorological data that allow parametrization of the physical processes occurring in the atmosphere. For this, the model uses 135 spectral intervals and 30 atmospheric layers for solving the radiative transfer equation. The interactions in the atmosphere between solar radiation and aerosols is one of the processes considered in the model by estimating the atmospheric transmittance from visibility values that are data inputs. As there are no measurements of visibility in Chile, its value is estimated in two steps: first, the visibility at sea level is computed as a function of latitude and date according to a standard atmosphere model, and then it is corrected by an exponential function in order to account for increased visibility at higher altitudes. In practice, the values used ranged from 5 to 150 km as for the original IGMK model (Stuhlmann et al., 1990) from which both the Brasil-SR and Chile-SR models are derived. Aerosols are the second most important parameter determining solar irradiance after clouds, as when under clear skies they become the main source of atmospheric extinction for DNI. If large errors in aerosol data ae present this results in DNI uncertainties that can be as large as 15–20% and up to 8% for GHI on a mean annual basis (Cebecauer

et al., 2011; Cebecauer and Suri, 2010; Gueymard, 2011). Several aerosol data sources show that for Chile the aerosol content in the atmosphere is minimum and thus it is considered there that the shortcomings of the visibility-based approach are minimized, which is supported by the relatively low error levels found in the model validation section (Cebecauer et al., 2011; Cebecauer and Suri, 2010; Gueymard, 2011; Aeronet program).

The Chile-SR model is made specific for the conditions of Chile by including updated altitude-corrected weather data (temperature, relative humidity, and atmospheric pressure), topography, and surface albedo. In addition, GOES images for visible and IR channels are used as input to first classify cloud types, and then determine an effective cloud cover. This step using both visible and IR channels is the main innovation over the existing Brasil-SR model, as it allows to solve the issues that arise from the particular geography of Chile where large salt lakes coexist with clouds and in turn both very close to snow covers, all of which appear as very similar in the visible channel. By adding the information given by the IR channel it is possible to differentiate clouds from ice and snow covers and from salt lakes. Additional details are provided in Escobar et al. (2014a).

Fig. 5 illustrates the sequence of main steps that Chile-SR takes in order to estimate radiation. Channel 1 (visible) and channel 4 (IR) from GOES images are utilized in order to identify and classify the type of cloud, which in turn helps determine the effective cloud cover that coupled to the atmospheric transmittance algorithm allows estimating the global horizontal irradiance. This picture also illustrates the additional difficulties that the research team has faced, in the form of salt lakes and snow covers that in a
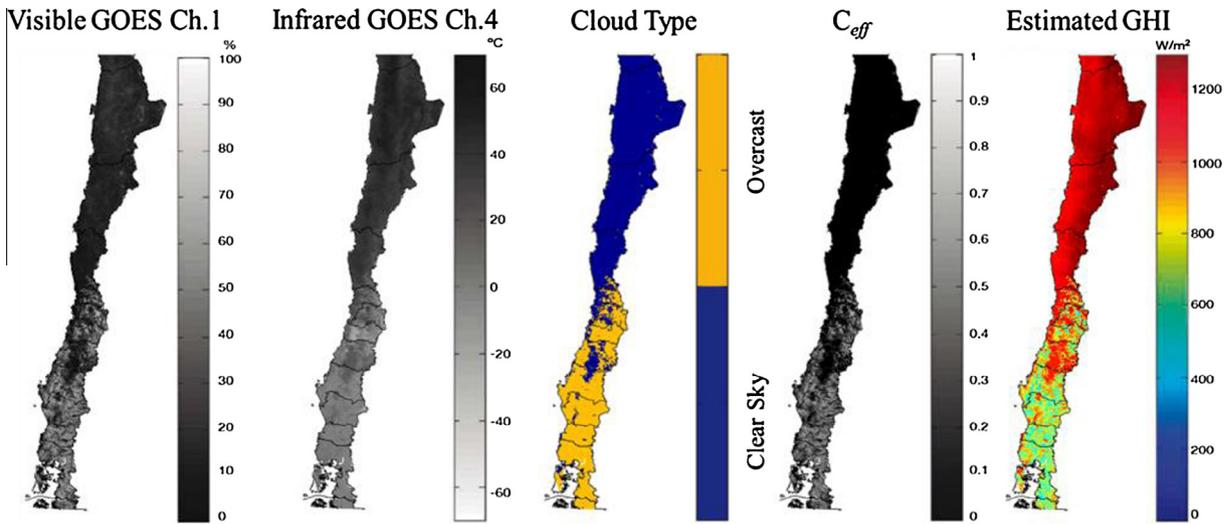
Fig. 5. Summarized procedure of the Chile-SR model: from visible and IR satellite images to estimated GHI.
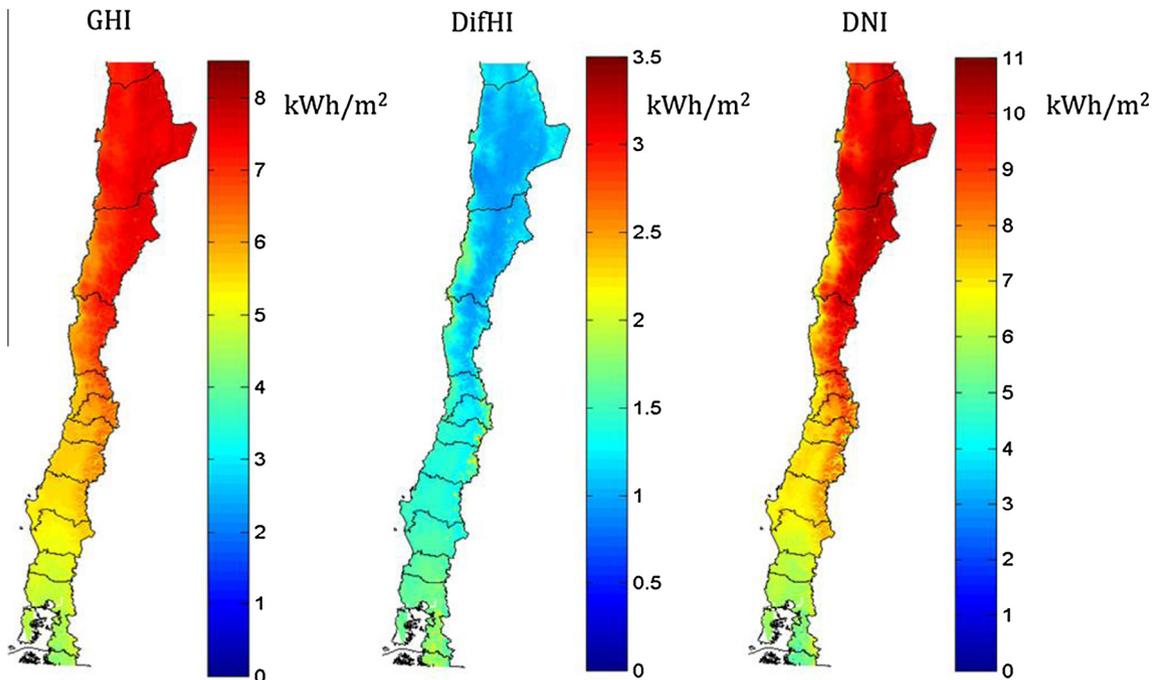
Fig. 6. Daily totals of radiation in yearly average for 2013.

visible channel picture might appear as cloud covers. The IR channel complements the visible channel image by giving information about the temperatures of each region. By properly combining the information from both channels, a cloud classification can be made, thus determining if a particular region is clear of clouds or if it has cloud covers. The next step is processing the cloud type and comparing the instantaneous information from each image to a monthly-established reference, which allows determining an effective cloud cover CCI_{eff}. In the particular situation depicted in Fig. 5 there are high values of GHI up to 1200 W/m^2 under clear skies, with cloud covers decreasing the GHI down to about 600 W/m^2.

As the output, data from the Chile-SR model is composed of only the GHI and direct horizontal radiation on an hourly basis, both the diffuse irradiance and the DNI must be computed from them. To this, the Boland–Ridley–Laurent (BRL) model of diffuse fraction is applied to the satellite-estimated GHI in order to compute the DNI. This model utilized multiple predictors for estimating the diffuse fraction DF using the hourly clearness index k_t, daily clearness index K_t, solar altitude α, apparent solar time AST and a measure of persistence ψ, which is an average of both a lag and a lead of the clearness index. According to Boland et al. (2013), Lauret et al. (2013), Ridley et al. (2010) this model performs substantially better

for Southern Hemisphere locations than other similar models. The BRL model was calibrated for Chile by using the ground station data in order to find the clearness index and persistence, and then applied to the satellite GHI data, which is used to compute the diffuse fraction and from that the direct horizontal irradiation and finally by considering the solar geometry it is possible to estimate the DNI. The best parameters for each location are selected by minimizing the sum of the square difference between the BRL-predicted diffuse fraction obtained with measured GHI, and the actual diffuse fraction obtained with the measured diffuse horizontal irradiance and the GHI.

Fig. 6 shows maps of daily irradiation in yearly average. It can be observed that daily totals over 5 kW h/m^2/day of GHI and over 6 kW h/m^2/day of DNI are present in most of the country, where the maximum levels reach over 8 kW h/m^2/day for GHI and 10 kW h/m^2/day for DNI. The highest values for GHI are found in northern Chile as the region shows low cloud cover presence and low aerosol contents, displaying values greater than 8 kW h/m^2/day in the intermediate depression and even higher in the Andes mountains. Locations in the intermediate depression of Chile between the coast and the Andes mountains present high values of GHI and DNI with a small decrease with latitude. The large influence of the coastal cloud covers are observed as radiation is much lower in the coast than in the intermediate depression, which in practice means that the technology options for coastal and interior northern Chile will be very different.

4. Comparison: Chile-SR satellite-derived data and ground stations

Fig. 7 shows the comparison for satellite-derived data and ground measurements for clear days in Crucero and Santiago. It can be observed that maximum levels for GHI at Crucero reach 1200 W/m^2, while at Santiago reach about 1165 W/m^2. This indicates that on clear days with similar atmospheric conditions, the available radiation in central Chile is comparable to that of northern Chile in terms of its magnitude. Figs. 3 and 6 have already shown that in clear days the conditions are very similar in Crucero and Santiago throughout the year and that in yearly totals the high radiation zones extend for most of the country

with minimum influence of the latitude. Although the actual conditions in any location are dependent on the specific atmospheric components for any given moment, it is nevertheless useful to point out that in general Central Chile has radiation levels which compare favorably to those of northern Chile, information which is relevant when planning country-wide promotion strategies for solar energy utilization. It can also be seen in Fig. 7 that good agreement between satellite estimations and ground measurements as found for clear days at the two different locations (desert and mediterranean climates).

Fig. 8 shows a comparison of satellite estimations and ground station data for daily totals combining the data available for all ground stations for the period 2010–2014. It is observed that there is good agreement between satellite and ground station data, resulting in an rRMSE of 8.9% when considering all stations as seen in Table 2. It can be noted that for values of irradiation lower than 3 kW h/m^2/day the satellite-derived data overestimates systematically the actual solar resource. For hourly average of irradiance comparison of satellite estimates and ground measurements (as in Fig. 8) the data have been separated into two geographical zones: (a) Northern Chile and (b) Central Chile. There is also a good agreement in an hourly basis, with a mean bias error (MBE) of 0.4% and a resulting rRMSE of 12.8%. The effect of overcast sky conditions (lower irradiance values) can be seen in both graph with a slightly overestimation of the model results. This phenomenon is greater in Central and Southern Chile, thus the rRMSE is higher than in Northern Chile, as it can be seen in Table 2. Finally, the KSI indicator (Kolmogorov–Smirnov test integral) and the OVER parameter are also evaluated as suggested in Espinar et al. (2009). There, the KSI parameter is defined as the integrated differences between the cumulative distribution functions (CDFs) of the two data sets (ground station and satellite estimation). The minimum value of the KSI index or percentage is zero, meaning that the CDFs of the two sets compared are equal. The OVER parameter indicates the area over the critical parameter of the KSI test and indicates how similar two data sets are regarding their respective CDFs.

The previous sections have shown first the details of the ground station network, then the Chile-SR model and the data it produces, and finally a comparison and validation
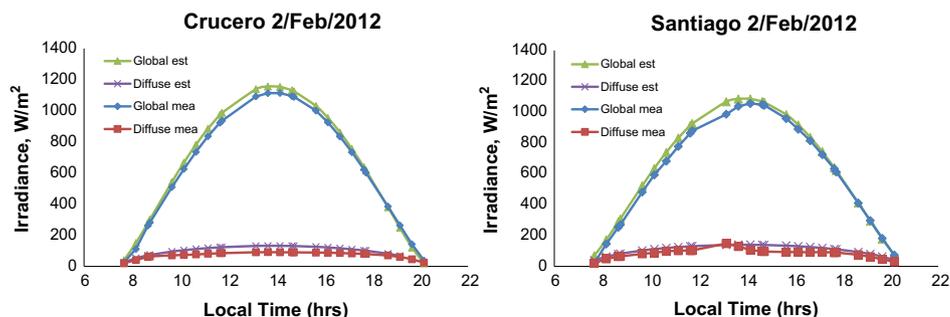
Fig. 7. Comparisons between satellite and ground data at Crucero and Santiago.
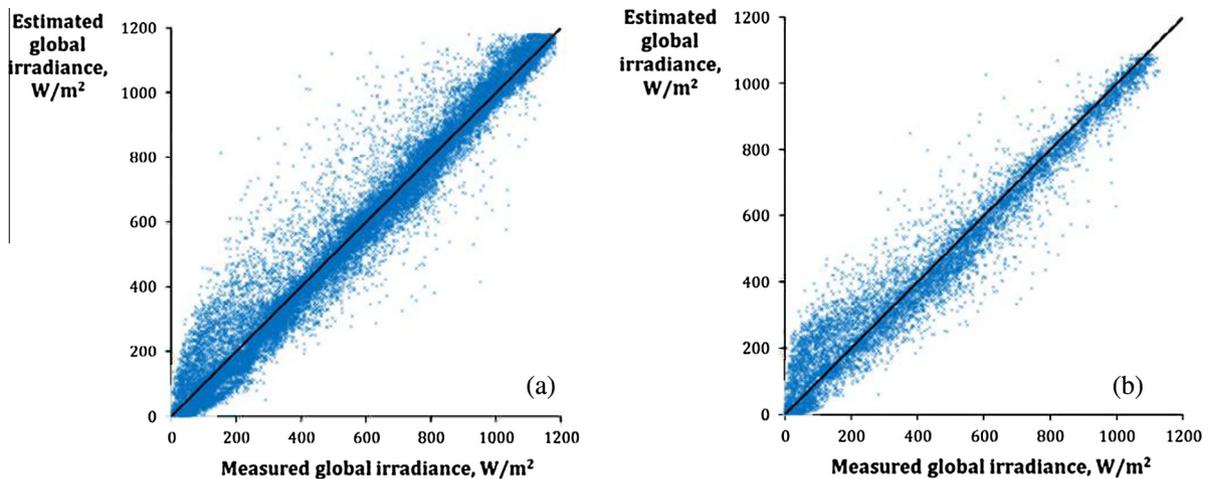
Fig. 8. Comparisons between satellite and ground data considering daily totals of irradiation. (a): Northern Chile. (b) Southern-Central Chile.

of the satellite estimations, concluding that Chile is endowed with a very high solar energy resource. In what follows, we will briefly describe the potential that Chile presents for utilizing solar energy, focusing on solar thermal, PV, and CSP systems.

5. Solar thermal energy applications for water heating

Approximately 91% of houses in Chile use gas heaters for residential water heating. The widespread use of this device is responsible for 18% of the energy consumed by the residential sector (MinEnergía-PNUD, 2012). The use of solar collectors can reduce the demand of imported fossil fuels. Currently there are approximately 139,309 m^2 of solar thermal collectors installed in Chile. Nevertheless, recent studies show that this number could be considerably increased in the next few years (Araya-Muñoz et al., 2014; Zalamea and Alvarado, 2014). In this context, using the detailed information obtained from Chile-SR model several simulations were carried out in order to assess the potential of solar thermal systems for supplying the residential energy demand in Chile. The potential was addressed in terms of the solar fraction, which represent the amount of energy delivered by the solar system, compared to the total energy demand. For that purpose, the f-chart algorithm was implemented (NREL, 2013; Duffie and Beckman, 2006), considering a conventional solar domestic hot water system consisting of a solar collector, either flat plate or evacuated tube, a circulation pump, a thermal storage system, and an auxiliary heater, as shown in Fig. 9. The residential water consumption was estimated considering the energy demand of a four people family, and assuming a daily hot water consumption rate of 75 l per person. The collector area is defined as 4 m^2, and the collectors are considered tilted towards the sun at an angle equivalent to the local latitude in order to maximize annual heat production. In order to estimate the incident radiation on a surface tilted towards the sun in such angle the Perez et al.

(1987) model was applied to the solar radiation database described in the previous sections.

One important issue related to solar water heating systems is *Legionnaires* disease. As well as temperature, the time taken for completely replace the volume of water held in the storage vessel is an important aspect. Research has shown that *legionella* bacteria dies in few minutes at 60 °C (IEA, 2001). Therefore, the storage tank volume was equivalent to the total water daily-consumed (300 l). Considering the aforementioned assumptions, the energy load for the solar thermal system is the energy required to raise tap water temperature to 40 °C. In this context, the tap water temperature for all the territory was estimated using the algorithm developed by Burch and Christensen (2007). This algorithm assumes that the temperature of the tap water depends on the ambient temperature and the annual thermal amplitude. Therefore, the energy load for water heating can vary according to the climatic features of each location. Therefore, considering the local ambient temperature and consumption temperature of 40 °C, the spatial distribution of the energy load for a dwelling house in Chile is shown in Fig. 10. The largest demands are observed at locations with high altitude, at the proximities of the Andes Mountains, since these areas are characterized by low ambient temperatures. On the other hand, coastal areas present higher temperatures and lower thermal amplitude, and consequently these areas present a lower energy load.

In order to assess the performance of the system using collectors with different characteristics, the simulations were carried out considering two collectors technologies: flat plate and evacuated tube. Additionally, considering the broad range of collectors available in the market, also two different collector efficiencies for each technologies were defined for high and low performance collectors as in Tables 3 and 4. Considering the parameters defined above the f-chart algorithm was used for estimating the potential contribution of solar systems for supplying the heat demand of dwellings, depending on the geographic location. That contribution was estimated using the solar

Table 2
Deviations observed for Chile-SR daily total irradiation and hourly averages irradiance estimates for each location of the ground stations.

	Daily total irradiation					Hourly average irradiance				
	MBE (kW h/m^2)	rMBE (%)	RMSE (kWh/m^2)	rRMSE (%)	KSI (%)	OVER (%)	MBE (W/m^2)	rMBE (%)	RMSE (W/m^2)	rRMSE (%)
Pozo Almonte	0.15	2.3	0.60	9.4	19.3	0.6	14.3	2.6	69.0	12.4
Sur Viejo	−0.20	−2.9	0.57	8.1	17.6	0.2	−16.1	−2.7	69.7	11.6
Crucero	−0.19	−2.7	0.55	7.9	11.4	0.9	6.1	1.0	62.9	10.4
Coya Sur	−0.09	−1.2	0.54	7.5	14.7	4.0	14.0	2.3	63.4	10.3
Diego de Almagro	−0.36	−4.5	0.56	7.1	15.3	0.4	−6.5	−1.0	53.8	8.3
Santiago	−0.01	−0.2	0.51	10.2	25.6	8.7	−0.3	−0.1	73.0	16.5
Curicó	−0.12	−2.7	0.65	14.6	31.3	14.0	22.1	5.7	92.8	24.0
Talca	−0.27	−4.8	0.64	11.2	28.5	16.0	6.1	1.3	87.4	18.9
Marimaura	−0.23	−0.1	0.79	19.8	27.5	24.9	4.8	1.4	86.0	24.0
Total	−0.13	−2.1	0.57	8.9	21.2	18.7	2.4	0.4	70.0	12.8

fraction as previously defined. Hence, the spatial distribution of the solar fraction operating with high and low performance flat plate and evacuated tube collectors is presented in Fig. 11. It is observed that as expected, the solar fraction in the northern region is higher than the solar fraction at southern locations. It is also observed that the coastal areas present higher solar fractions than the mountain regions (at the same latitude). This situation is noteworthy since at the coastal regions of Chile it is common to observe thick clouds events during the morning, which decrease the availability of solar radiation. Nonetheless, the high thermal amplitude observed on the desert and mountain areas increases significantly the energy load, which reduces the solar fraction. According to the results depicted in Fig. 11, the reduction on the efficiency of the collectors affects significantly the energy supplied by the system. It is worth mentioning that the high performance collector allows reaching solar fractions over 65% throughout all the populated areas of the country, even in mountain regions. Particularly in the northern region, where the populated areas are located close to the ocean, the flat plate collectors can supply almost 90% of the energy load. Furthermore, in the city of Calama, located in the desert close to the mining facilities, the solar Fraction achieves values close to 95%.

6. Photovoltaic applications

Cost reductions for photovoltaic systems have sparked massive interest in Chile for its application in both: large scale power plants and distributed generation. In order to assess the potential yield of a generic PV system, the solar radiation database derived from the Chile-SR model was utilized, using the Perez model for estimation the incident radiation in a tilted surface (Perez et al., 1987). Therefore, the potential yield was estimated through simulations developed using the PVWatts algorithm (SAM, 2014) and considering latitude-tilted modules, thus the results are presented in terms of the equivalent peak hours kW h/kWp, which indicate the specific yield of a system regardless of the technology employed. Fig. 11 displays the results for

this analysis. as observed Daily yield decreases with latitude as expected, and coastal locations display a lower yield due to the increased atmospheric thickness at sea level and due to the presence of early morning cloud formations typical of the Chilean coast as previously discussed (Cereceda et al., 2008). Best yields are located in the Atacama desert region, starting about 5–20 km from the coast and at altitudes higher than 1000 m over sea level. The highest yields are almost as high as 8 kW h/kWp. It is worth noting that high yields are observed in a vast extension of territory, as far south as the mountains close to Santiago.

7. Concentrated solar power plants

Several studies have indicated the CSP technologies as a reliable alternative to meet part of the growing electric demand in the future (IEA, 2012; Sarge and Lundy Consulting Group, 2003). The CSP systems are composed of a concentrator solar field, thermal receivers, transport and storage of thermal fluid, and a power cycle. The concentrated radiation is absorbed by the receiver, achieving temperatures up to 600 °C, and then, the heat absorbed by the working fluid is then used to drive a conventional power cycle. Within the CSP technologies available today,
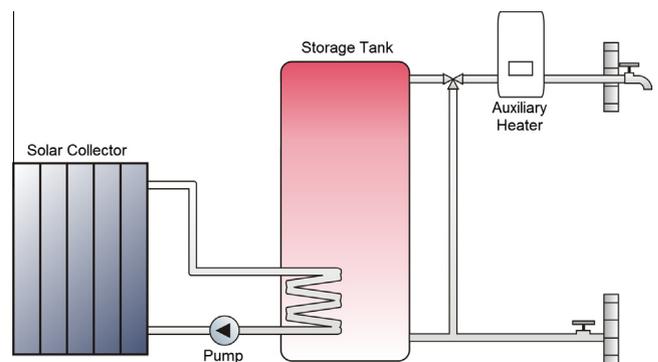
Fig. 9. Solar system configuration for residential water consumption scenario.
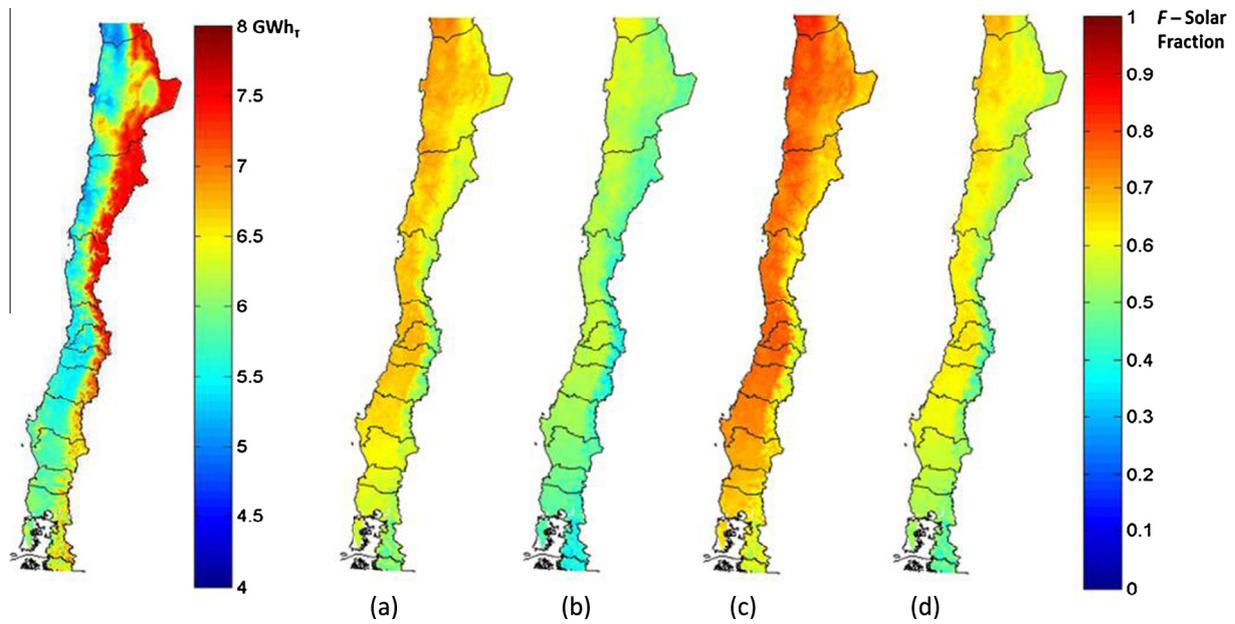
Fig. 10. Annual energy load for residential water heating, as function of the geographic location, in GW h (left), and annual solar fraction using (a) high performance; (b) low performance flat plate solar collectors; (c) high performance, (d) low performance evacuated tube collector.

parabolic trough collectors is the most developed. The main requirement for developing projects concerning CSP technologies is a high availability of direct solar radiation, proximity to the distribution grid and the availability of relatively flat areas (IEA, 2012). In this context, considering the information obtained by the Chile-SR model combined with geographical information about the altitude, was possible to identify the feasible locations for the deployment of CSP plants in the Chilean territory. The locations present a slope lower than 3% and an annual DNI higher than 2100 kW h/m^2 (IEA, 2012). The sites that meet the specified conditions are not restricted to the northern region of Chile in the Atacama desert area yet extend along the country until 36°S. However, the highly variable solar resource during the year and the alternative

uses of land for agricultural purposes, limits the potential application of CSP plants in central Chile, from 30°S to further south. Several simulations were carried out considering the parabolic trough technology in order to assess the performance of such systems if they were operating under the Chilean metheorological conditions. From that simulations, four locations were selected in order to demonstrate the feasibility of operating CSP plants in different regions of the country: Crucero, Diego de Almagro (26,4°S; 70°W), Santiago and Curicó. The simulations were carried out using the System Advisor Model software (SAM, 2014) and an hourly solar radiation database, constructed using the results of the Chile-SR model. The analysis considers the operation of a parabolic trough plant with analogous configuration to the ANDASOL 1 solar power plant located in Granada, Spain. This plant has a nominal capacity of 50 MW with 510,120 m^2 of aperture area and 7.5 h of thermal energy storage.

Fig. 12 shows the results of the simulations in terms of the monthly net energy output for the four selected locations. Although at Crucero and Diego de Almagro it is observed a seasonal variation on the energy generation, it is not as severe as observed for Santiago and Curicó. It should be noted that the annual net energy generation for the first two locations is 50% higher than the energy output of the reference plant, ANDASOL 1 (158 GW h) NREL, 2013; Duffie and Beckman, 2006. In fact, the energy delivered by ANDASOL is equivalent to the energy generation expected for a plant installed in Santiago. The radiation conditions of Northern Chile make it possible to reduce the investment costs associated to the solar field, since smaller collecting areas are needed for an equivalent power production capacity.

Table 3
Efficiency parameters of the flat plate collectors considered in the simulations.

	High performance collector	Low performance collector
$F_R (\tau\alpha)$	0.789	0.734
$F_R U_L$	4.360	5.250
$K_{(\tau\alpha)}$	0.954	0.855

Table 4
Efficiency parameters of the evacuated tube collectors considered in the simulations.

	High performance collector	Low performance collector
$F_R (\tau\alpha)$	0.79	0.68
$F_R U_L$	1.58	2.94
$K_{(\tau\alpha)}$	0.95	0.94
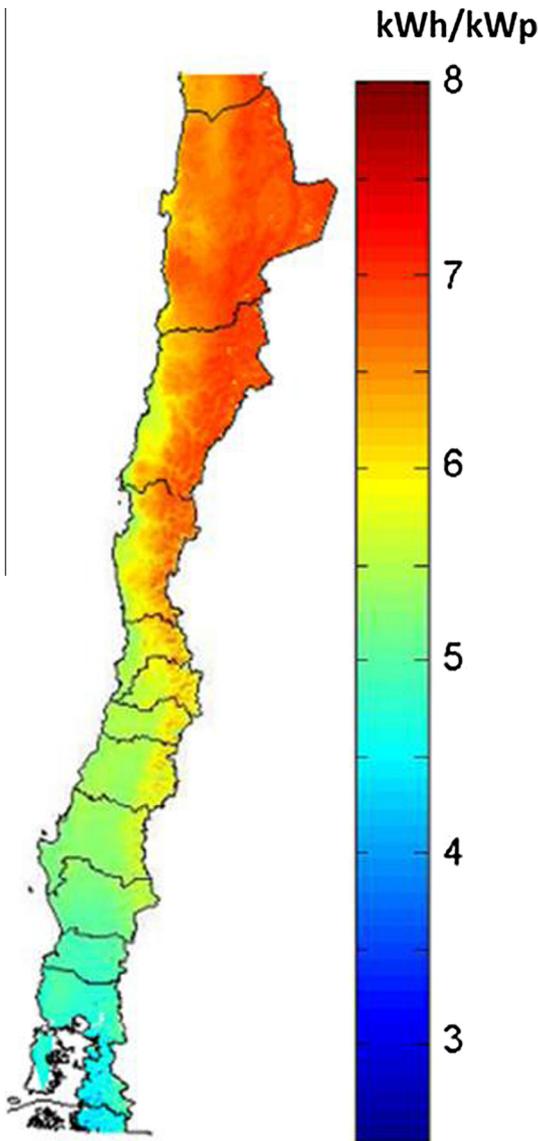
Fig. 11. Specific daily yield of PV systems in Chile in yearly average.
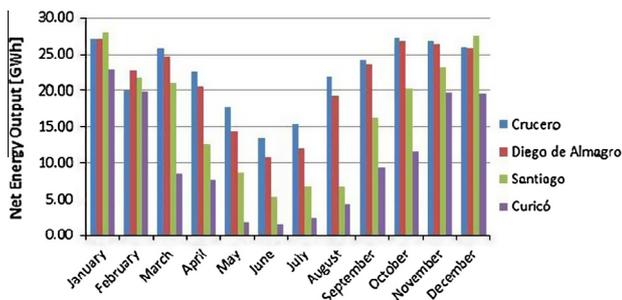
Fig. 12. Monthly net energy output of a parabolic trough plant for the selected locations.

8. Conclusions

Renewable Energy promotion efforts in Chile aim to achieve a power production quota of 10% to be met by 2024. This plan has sparked interest in solar energy among other renewable sources, with PV, CSP, and industrial heat supply plants being announced. Previous reports by the authors have identified several databases of solar radiation finding that significant deviation exists between sources, with most data from ground station measurements displaying unknown uncertainty levels, which highlighted the need for a proper, country-wide long-term resource assessment initiative. This report updates the situation in Chile by considering the efforts performed in the last five years by a resource assessment program based on the development of a satellite estimation model, complemented by a modern measurement ground station network. The PUC-FONDEF program has deployed a network of twelve ground stations which are producing data according to international standard and good practices. A satellite estimation model has been developed to account for the particular conditions found in Chile and validated with data from the ground stations achieving good agreement with average rRMSE of 8.9%. The results indicate that Chile is endowed with one of the highest solar highest level of solar resource in the world. The use of the Chile-SR irradiation data for system simulations indicates that solar fractions over 80% are achievable for solar thermal systems in most of the country, with PV systems yielding between 4.5 and 8 kW h/kWpv and CSP annual yields of up to 240 GW h/year for a 50 MW parabolic trough plant. Population and industry centers in Chile are located in regions where the solar irradiation and the potential for its utilization are high, thus indicating that the country could develop promotion schemes for solar energy systems in order to decrease its energy dependence upon foreign imports of fossil fuels.

References

Aeronet program: <http://aeronet.gsfc.nasa.gov/>.

Araya-Muñoz, D., Carvajal, D., Sáez-Carreño, A., Bensaid, S., Soto-Márquez, E., 2014. Assessing the solar potential of roofs in Valparaíso (Chile). Energy Build. 69, 62–73.

Boland, John, Huang, Jing, Ridley, Barbara, 2013. Decomposing global solar radiation into its direct and diffuse components. Renew. Sustain. Energy Rev. 28, 749–756.

Burch, J., Christensen, C., 2007. Towards development of an algorithm for mains water temperature. In: Proceedings of the Solar 2007 Conference, 8–12 July 2007, Cleveland, Ohio.

Cebecauer, T., M., Suri., 2010, Accuracy improvements of satellite-derived solar resource based on GEMS re-analysis aerosols. In: Proc. Conf. SolarPACES 2010, Perpignan, France.

Cebecauer, T., Suri, M., Gueymard, C., 2011. Uncertainty sources in satellite-derived direct normal irradiance: how can prediction accuracy be improved globally? In: Proceedings of the SolarPACES Conference, Granada, Spain, 20–23 September 2011.

Cereceda, P., Larrain, H., Osses, P., Farías, M., Egaña, I., 2008. The climate of the coast and fog zone in the Atacama Desert of Tarapacá Region, Chile. Atmos. Res. 67 (3–4), 301–311.

CIFES, 2014. Report from Center for Innovation and Support of Sustainable Energy (CIFES), Chile, December 2014 and June 2015. <http://www.cifes.gob.cl/ (accessed 30.07.20).

Duffie, J.A., Beckman, W.A., 2006. Solar Engineering of Thermal Processes, third ed. John Wiley and Sons, New Jersey.

Escobar, R., Cortés, C., Pino, A., Pereira, Enio Bueno, Martins, F., Cardemil, J., 2014a. Solar energy resource assessment in Chile: satellite estimation and ground station measurements. Renew. Energy 71, 324–332.

Escobar, R., Ortega, A., Cortés, C., Pino, A., Pereira, E. Bueno, Ramos Martins, F., Boland, J., 2014b. Solar energy resource assessment in Chile: satellite estimation and ground station measurement. Energy Proc. 57, 1257–1265.

Espinar, Ramírez, Drews, Beyer, Zarzalejo, Polo, et al., 2009. Analysis of different comparison parameters applied to solar radiation data from satellite German radiometric stations. Sol. Energy 83, 118–125.

Gueymard, C.A., 2011. Uncertainties in modeled direct irradiance around the Sahara as affected by aerosols: are current datasets of bankable quality? J. Sol. Energy Eng. 133 (3), 031024.

Habte, A., Sengupta, M., Reda, I., Andreas. A., 2014. Calibration and measurement uncertainty estimation of radiometric data. Solar 2014, San Francisco, California, July 6–10.

Hegner, H., Müller, G., Nespor, V., Ohmura, A., Steigrad, R., Gilgen, H., 1998: Update of the technical plan for BSRN data management. WMO/TD-No. 882, WCRP/WMO (accessed 30.07.15).

IEA, 2001. Proceedings of the Legionella Workshop. Paris, International Energy Agency, 52p.

IEA, 2012. Concentrated solar power technology roadmap. International Energy Agency.

JCGM, 2008. Guide to the expression of uncertainty in measurement. Working Group 1 of the Joint Committee for Guides in Metrology. <http://www.bipm.org/utils/common/documents/jcgm/JCGM_100_2008_E.pdf>.

König-Langlo, G., Sieger, R., Schmithüsen, H., Bücker, A., Richter, F., Dutton, E.G., 2013: The Baseline Surface Radiation Network and Its World Radiation Monitoring Centre at the Alfred Wegener Institute. <www.wmo.int/pages/prog/gcos/Publications/gcos-174.pdf> (accessed 30.07.15).

Lauret, Philippe, Boland, John, Ridley, Barbara, 2013. Bayesian statistical analysis applied to solar radiation modelling. Renew. Energy 49, 124–127.

Martins, F., Pereira, E.B., Abreu, S., 2007. Satellite-derived solar resource maps for Brasil under SWERA project. Sol. Energy 81, 517–528.

Martins, F., Pereira, E.B., Silva, S., Abreu, S., Colle, S., 2008. Solar energy scenarios in Brasil, Part one: Resource assessment. Energy Pol. 36, 2853–2864.

MAuthner, F., Weissm, W., Spörk-Dür, M., 2015. Solar Heat Worldwide 2015 edition. International Energy Agency. <http://www.iea-shc.org/data/sites/1/publications/Solar-Heat-Worldwide-2015.pdf>.

McArthur, L.J.B., 2004. Baseline Surface Radiation Network (BSRN). Operations Manual. WMO/TD-No. 1274, WCRP/WMO (accessed 30.07. 2015).

MinEnergía-PNUD, 2012. Estudio de mercado de la industria solar térmica en Chile y la pro-puesta metodológica para su actualización permanente. Santiago, Chile.

Ministerio de Economía de Chile, 2007. Ley general de servicios eléctricos, Decreto con fuerza de ley n 4, Art. único N° 2, D.O. 01.04.2008.

Myers, Daryl R., Stoffel, Thomas L., Reda, Ibrahim, Wilcox, Stephen M., Andreas, Afshin M., 2001. Recent progress in reducing the uncertainty in and improving pyranometer calibrations. J. Sol. Energy Eng. 124 (1), 44–50.

NREL, 2013. System advisor model (SAM) Case study: andasol-1.

Ortega, A., Escobar, R., Colle, S., Luna de Abreu, S., 2010. The state of solar energy resource assessment in Chile. Renew. Energy 35 (11), 2514–2524.

Pereira, E., Martins, F., de Abreu, S., Ruther, R., 2006. Atlas Brasilero de Energía Solar. INPE.

Perez, R., Seals, R., Ineichen, P., Stewart, R., Menicucci, D., 1987. A new simplified version of the Perez diffuse irradiance model for tilted surfaces. Sol. Energy 39, 221–232.

Reda, I., 2011. Method to Calculate Uncertainty Estimate of Measuring Shortwave Solar Irradiance Using Thermopile and Semiconductor Solar Radiometers. NREL/TP-3B10-52194, Golden, CO, National Renewable Energy Laboratory.

Ridley, Barbara, Boland, John, Lauret, Philippe, 2010. Modelling of diffuse solar fraction with multiple predictors. Renew. Energy 35, 478–483.

Ruther, R., Abreu, S., Pereira, E.B., 2008. Solar energy scenarios in Brasil, Part two: Photovoltaics applications. Energy Pol. 36, 2865–2877.

SAM, 2014. System advisor model version 2015.1.30 (SAM 2014.1.30) user documentation. Sizing the Flat Plate PV System. National Renewable Energy Laboratory. Golden CO.

Sargent & Lundy Consulting Group, 2003. Assessment of parabolic trough and power tower solar technology cost and performance forecasts. Report SL-5641 prepared for National Renewable Energy Laboratory and US Department of Energy.

Stuhlmann, R., Rieland, M., Raschke, E., 1990. An improvement of the IGMK model to derive total and diffuse solar radiation at the surface from satellite data. J. Appl. Meteorol. 29, 586–603.

Zalamea, E., Alvarado, R.G., 2014. Roof characteristics for integrated solar collection in dwellings of real- estate developments in Concepcion, Chile. J. Constr. 13 (3), 36–44.